energies

MDPI

Article

Surface Complexation Modelling of Wettability Alteration during Carbonated Water Flooding

Fagan Mehdiyev [1], Samuel Erzuah [2], Aruoture Omekeh [3] and Ingebret Fjelde [3,*]

[1] Department of Energy and Petroleum Engineering, University of Stavanger (UiS), 4021 Stavanger, Norway; faganmehdiyev96@gmail.com
[2] Department of Petroleum Engineering, Kwame Nkrumah University of Science & Technology (KNUST), Kumasi 00233, Ghana; samuel.erzuah@knust.edu.gh
[3] Department of Energy & Technology, NORCE Norwegian Research Centre AS, 4021 Stavanger, Norway; arom@norceresearch.no
* Correspondence: infj@norceresearch.no

Abstract: CO_2 capture and utilization is an effective tool in reducing greenhouse gas emissions and hence, combating global warming. In the present study, surface complexation modeling (SCM) with the geochemistry solver, PHREEQ-C, was utilized to predict the wettability alteration of minerals, sandstone reservoir rocks (SRR), and pseudo-sandstone rocks (PSR) and mineral mixtures during carbonated water (CW) injection. The bond products, which is defined as the product of the mole fraction of oppositely charged mineral and oil surfaces, were calculated to estimate the wettability preferences. For the studied fluid systems, the results from SCM predicted that albite and quartz minerals were strongly water-wet while calcite was strongly oil-wet with formation water (FW). When it came to clay minerals, illite and montmorillonite were more oil-wet than quartz and less oil-wet than calcite. During CW injection (CWI), the wettability preferences of dominant minerals (considering weight and surface area) in SRR (i.e., quartz and calcite) were changed toward more water-wet, while for the clay minerals, the result was the opposite. The results from SCM showed that the wettability preferences of SRR were water-wet in both CW and FW. Moreover, increasing the amount of the water-wet minerals in mineral mixtures increased the rock's tendency to become more water-wet.

Keywords: wettability alteration; carbonated water; surface complexation modelling; improved oil recovery; CO_2 utilization

Citation: Mehdiyev, F.; Erzuah, S.; Omekeh, A.; Fjelde, I. Surface Complexation Modelling of Wettability Alteration during Carbonated Water Flooding. *Energies* **2022**, *15*, 3020. https://doi.org/10.3390/en15093020

Academic Editors: Kun Sang Lee and Riyaz Kharrat

Received: 17 January 2022
Accepted: 7 April 2022
Published: 20 April 2022

1. Introduction

Wettability is the tendency of a fluid to adhere to a solid surface in the presence of other immiscible fluids [1]. In oil reservoirs, wettability is important for the multiphase flow because it affects the fluid phase distribution and flow properties in the oil reservoirs. For instance, research has shown that early water breakthrough occurs in hydrophobic media as compared to hydrophilic media [2]. Numerous techniques have been used to characterize wettability and wettability alteration, e.g., Amott test [3], United States bureau of mines (USBM) method [3,4], and flotation technique [3,5–7]. In the Amott test, the wettability is determined by measuring the volume of fluid (water and oil) spontaneously and forcibly imbibed by a core plug while in the USBM method, the area under the capillary pressure curve is used to determine the work required to do the forced displacement. In the flotation tests, the wettability is characterized by the affinity of the rock or mineral samples to either the oil or the brine. Research has also shown that increasing the water-wetness of the rock surface tends to increase and/or accelerate oil recovery [2]. There are numerous techniques of altering the wettability, notably low salinity water flooding (LSWF) [8], smart water injection [9], and carbonated water injection [10]. In this study, the potential for wettability alteration of sandstone reservoir rocks by carbonated water flooding (CWF) was

estimated using surface complexation modelling (SCM). Compared to other methods for wettability determination (e.g., the Amott and the USBM), the SCM technique is fast and experiments are not required. SCM can also predict the oil adhesion mechanisms such as direct adhesion of carboxylate (>COO^-) and cation bridging.

Carbonated water (CW) has successfully been used to increase the oil recovery efficiency in laboratory studies [10]. CW can be prepared either by co-injection of carbon dioxide (CO_2) and brine or via water alternating CO_2 (CO_2-WAG) injection. It has been reported in the literature that the increase in oil recovery during the CWF is attributed to the following mechanisms:

- Reduction of the oil-water interfacial tension [11,12];
- Reduction of the oil viscosity [11,13,14];
- Oil swelling due to CO_2 diffusion into the oil phase [11,15]; and
- Wettability alteration [11,16–18].

Other mechanisms that have also been reported to be responsible for the increase in oil recovery during CWF include solution gas drive [12], coalescence of oil ganglia [15], and new gaseous phase formation [17,19]. These mechanisms are hinged on the diffusion of CO_2 from CW to either dissolve in the oil phase to form solution gas or exist as free gas inside the reservoir.

SCM has proved useful in understanding the mechanisms in wettability alterations for low salinity water [20–23], smart water [24], and carbonated water in calcite in more recent studies [25,26]. SCM has successfully been used to capture the trend for some laboratory measurements such as flotation test, zeta potential (ζ-potential), and recently contact angle measurements [21,27,28]. It has been reported in the literature that the ionic composition of the brine and brine pH, the surface charge of the mineral or rock, and the surface-active oil components influence the wetting state [29].

Numerous SCM models exist, namely: constant capacitance, diffuse-layer, triple-layer, and two-pK models [30]. The differences in these models are hinged on the assumptions surrounding the choice of surface sites, the calculation of the electric potential (Ψ), and the description of the electric double layer [31]. SCM capitalizes on the thermodynamic properties of the surfaces involved (i.e., oil and mineral) to model their surface reaction during the experiment [30,32]. The equilibrium constant for adsorption, protonation, and deprotonation are some of the thermodynamic properties needed to model these interactions [20,30]. Other parameters such as surface site densities and surface area are needed to successfully model the interactions [20,30].

There are number of crude oil, brine, and rock (COBR) interactions taking place in the reservoirs as a result of the different properties of the surfaces involved (e.g., crude oil, brine, and rock). Surface reactions and equilibrium reaction constants of mineral and brine systems have been well studied [20,32–34]. The surface reaction of oil and their reaction constants with different brines have also been reported in the literature [20,32]. These reported thermodynamic properties from the literature were used as input in the SCM to model the COBR interactions [27]. The wettability of quartz, kaolinite, and calcite has also been predicted in the literature using the SCM [27] by relying on the existing reported data [20,34–36]. This was achieved by assessing the attractive electrostatic forces existing between the oil and brine and mineral and brine interfaces via SCM.

The present study is based on a previous manuscript [37] and master thesis [38]. The objective was to determine the wettability alteration potential of carbonated water injection (CWI) on selected minerals, sandstone reservoir rocks, and pseudo-sandstone rocks (crushed sandstone rock with added minerals). This has established better understanding of the impact of brines (i.e., formation water and carbonated water) and intrinsic parameters on the wettability of the reservoirs. In other words, the electrostatic pair linkages existing between the rock–brine and the oil–brine interfaces were evaluated to better understand the role of CW in wettability alteration.

2. Method Surface Complexation Modelling

SCM technique has been very useful in the modelling of solutes' adsorption from aqueous solutions to minerals [39]. It is a relatively economical and quick method for determining the wetting state of minerals and reservoir rocks and can be used as a screening tool to estimate the wettability alteration potential of CW in reservoir rocks. For promising reservoirs, laboratory experiments and reservoir simulations should be performed. Input parameters to the simulations are below first presented for the individual minerals, mineralogical composition of the reservoir rocks, and mineral mixtures. The properties of fluids (brine types and STO) are then given in tables. The SCM method is also briefly described to present the working principle. A more complete description can be found in previous publication [27].

2.1. SCM Input

Two sandstone reservoir rocks and their dominant mineralogical constituents, namely quartz, albite, montmorillonite, illite, and calcite were used. To add to the above, four mineral mixtures were designed by increasing the content of either illite or calcite in the sandstone reservoir rocks. Throughout this study, the two sandstone reservoir rocks are denoted by SRR#1 and SRR#2 while the mineral mixtures (pseudo-sandstone rock) is denoted as PSR. It is worth noting that the concentration of illite was increased in PSR#1 and PSR#2, while PSR#3 and PSR#4 were designed by increasing calcite content. Table 1 gives the mineralogical compositions of the sandstone rocks used in the simulation.

Table 1. Mineralogical compositions (weight percent) of the sandstone rocks and the mineral mixtures.

Mineral	SRR#1	SRR#2	PSR#1	PSR#2	PSR#3	PSR#4
Quartz	83.7	94.9	62.8	41.9	62.8	41.9
Albite	3.3	4.0	2.5	1.6	2.5	1.6
Montmorillonite	3.9	0.0	2.9	1.9	2.9	1.9
Illite	8.8	0.4	31.6	54.4	6.6	4.4
Siderite	0.0	0.5	0.0	0.0	0.0	0.0
Calcite	0.3	0.2	0.2	0.2	25.2	50.2

The compositions of stock tank oils (STO) and the formation waters (FW) used in the simulation are given in Tables 2 and 3, respectively. The initial pH of the brine is given as an input in the model and the final pH is then determined by the interactions that are simulated. Input parameters of CW were obtained by dissolving CO_2 in the FW to form CW with a CO_2 content of 2 mmol/L [38].

Table 2. Total acid number (TAN), total base number (TBN), and density of the stock tank oils (STO).

Fluid	Density (g/cm^3)@ 20 °C	TAN (mg KOH/g Oil)	TBN (mg KOH/g Oil)
STO #1	0.86	0.10	1.90
STO #2	0.90	0.38	2.30

2.2. Bond Product and Total Bond Product

The oil adhesion based on the attractive electrostatic forces existing between the rock–brine and the oil–brine interfaces is represented by the bond product (*BP*) [20,27]. *BP* is the product of the mole fractions of the oil (O_i) and mineral (m_i) sites with unlike charges [27] and it is given by the Equation:

$$BP = O_i m_i \quad (1)$$

Table 3. Ionic compositions of used brines.

ION	FW#1 (mmol/L)	FW#2 (mmol/L)	CW #1 (mmol/L)	CW #2 (mmol/L)
Na^+	1326.16	701.88	1326.16	701.88
K^+	5.62	7.11	5.62	7.11
Mg^{2+}	17.46	23.90	17.46	23.90
Ca^{2+}	147.94	72.85	147.94	72.85
Sr^{2+}	8.44	1.65	8.44	1.65
Ba^{2+}	0.00	0.04	0.00	0.04
Cl^-	1677.67	898.69	1677.67	898.69
SO_4^{2-}	0.89	3.59	0.89	3.59
HCO_3^-	**0**	**0**	**2**	**2**
pH	**5.90**	**5.87**	*	*
Density (g/cm^3) at 20 °C	1.07	1.04	1.07	1.04

* Final pH is determined by simulation of the interactions in the fluid-mineral and rock systems.

For a given mineral or rock, the sum of all the *BP* is the total bond product (*TBP*) [27]. The SCM predicts the oil adhesion onto a mineral or rock surface using the electrostatic pair linkages existing between the mineral–brine and oil–brine interfaces during COBR interactions (Figure 1). It has been reported in the literature that the higher the *TBP*, the higher the tendency for oil to be adsorbed onto the surface and opposite [27]. From Figure 1, the ">" represents the surface groups (i.e., oil and mineral groups). From literature [27], the TBP can be written as:

$$TBP = \sum_i^n BP_i \quad (2)$$

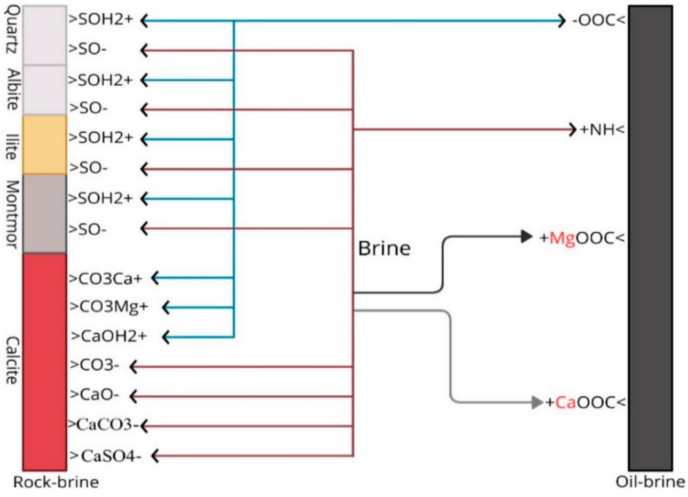

Figure 1. The electrostatic pair linkages between the rock–brine and oil–brine interfaces with unlike charges are given. Direct adsorption of carboxylate (>COO-) onto the positive mineral sites (>SOH_2^+, >CO_3Ca^+, >CO_3Mg^+, and >$CaOH_2^+$) can lead to oil adsorption [37].

The surface-active components in the crude oil were depicted by their respective acidic (>COOH) and basic oil (>NH^+) groups, while the minerals (rocks) were represented by their mineral sites (e.g., >Si-O-H, >CO_3H, and >CaOH). The oil surface reactions and their reaction constants were obtained using similar data from literature [20]. To add to the above, the surface reactions of the studied minerals and their reaction constants were also obtained from literature as depicted in Table 4. For the PSR, the thermodynamic properties of their individual mineralogical constituents were used. However, since each mineralogical constituent of the PSR has a unique reactive surface area, the effective surface area of the PSR was calculated using the Equation:

$$A_{eff} = \sum_{n=1}^{\infty} m_i \, A_i, \quad (3)$$

where,

A_{eff} = Effective surface area (m^2/g);

m_i = Mass fraction of mineral i (dimensionless); and

A_i = Reactive surface area of mineral i (m^2/g).

From literature [27], the properties of the STO such as the TAN and TBN were converted to their respective oil site densities and used as input into the SCM:

$$\text{Oil Site Density}\left(\text{site}/\text{nm}^2\right) = \frac{\text{TAN or TBN}(\text{mg KOH}/\text{g oil})}{\text{Mw KOH}\ (\text{g}/\text{mol})} \times \frac{\text{Avogadros Constant}}{\text{Effective Surface Area}\ (\text{m}^2/\text{g})} \quad (4)$$

The thermodynamic properties of the surfaces (i.e., oil and mineral surfaces) as reported in the literature can be obtained from Table 4. The site densities and surface area of the minerals as reported in the literature can be found in Table 5. Note that the reactive surface area may not necessarily be the total surface area of the mineral, e.g., the used reactive surface area for montmorillonite represents only the area that is variable charged (edged surface) [40]. Similar views have been expressed by others [41] where it was reported the actual contact area between crude oil and rock is much smaller than the apparent contact area.

Table 4. SCM input parameters.

Reaction	log K @ 25 °C	Enthalpy (KJ/mol)
[a] **Oil Surface**		
$>NH^+ \leftrightarrow\boxed{} >N + H^+$	−6.0	34.0
$>COOH \leftrightarrow\boxed{} >COO^- + H^+$	−5.0	0.0
$>COOH + Ca^{2+} \leftrightarrow\boxed{} >COOCa^+ + H^+$	−3.8	1.2
$>COOH + Mg^{2+} \leftrightarrow\boxed{} >COOMg^+ + H^+$	−4.0	1.2 [g]
[b] **Quartz**		
$>Si\text{-}O\text{-}H + H^+ \leftrightarrow\boxed{} >Si\text{-}O\text{-}H_2^+$	−1.1	−26.4
$>Si\text{-}O\text{-}H \leftrightarrow\boxed{} >Si\text{-}O^- + H^+$	−8.1	8.4
[c] **Albite**		
$>Si\text{-}O\text{-}H + H^+ \leftrightarrow\boxed{} >Si\text{-}O\text{-}H_2^+$	1.9	16.3
$>Si\text{-}O\text{-}H \leftrightarrow\boxed{} >Si\text{-}O^- + H^+$	−8.5	1.3
[d] **Illite**		
$>Si\text{-}O\text{-}H + H^+ \leftrightarrow\boxed{} >Si\text{-}O\text{-}H_2^+$	7.43	24.3 [h]
$>Si\text{-}O\text{-}H \leftrightarrow\boxed{} >Si\text{-}O^- + H^+$	−8.99	18.8 [h]
$H^+ + NaX_{ill} \leftrightarrow\boxed{} HX_{ill} + Na^+$	1.6	0.0
[e] **Montmorillonite**		
$>Si\text{-}O\text{-}H + H^+ \leftrightarrow\boxed{} >Si\text{-}O\text{-}H_2^+$	5.4	24.3 [h]
$>Si\text{-}O\text{-}H \leftrightarrow\boxed{} >Si\text{-}O^- + H^+$	−6.7	18.8 [h]
$H^+ + NaX_m \leftrightarrow\boxed{} HX_m + Na^+$	4.6	0.0
[f] **Calcite**		
$>CO_3H \leftrightarrow\boxed{} >CO_3^- + H^+$	−4.9	−5.0
$>CO_3H + Ca^{2+} \leftrightarrow\boxed{} >CO_3Ca^+ + H^+$	−2.8	25.7
$>CO_3H + Mg^{2+} \leftrightarrow\boxed{} >CO_3Mg^+ + H^+$	−2.2	4.5
$>CaOH + H^+ \leftrightarrow\boxed{} >CaOH_2^+$	12.2	−77.5
$>CaOH \leftrightarrow\boxed{} >CaO^- + H^+$	−17.0	116.4
$>CaOH + 2H^+ + CO_3^{2-} \leftrightarrow\boxed{} >CaHCO_3 + H_2O$	24.2	−90.7
$>CaOH + CO_3^{2-} + H^+ \leftrightarrow\boxed{} >CaCO_3^- + H_2O$	15.5	−61.6
$>CaOH + SO_4^{2-} + H^+ \leftrightarrow\boxed{} >CaSO_4^- + H_2O$	13.9	−72.0

[a] after [20], [b] and [c] after [31,35], [d] after [33], [e] after [40], [f] after [34], [g] enthalpy for reaction between >COOH and Mg^{2+} was assumed to be the same as Ca^{2+} [h] which assumed same enthalpy as kaolinite reactions. Note. X_{ill} and X_m depict the exchange sites of illite and montmorillonite, respectively.

Table 5. Properties of the minerals and reservoir rocks.

Surface	Site Density (site/nm^2)	Effective Surface Area (m^2/g)
Quartz	10.00	1.20
Albite	1.155	1.20
Illite	1.37	66.8
Montmorillonite	5.7	3.0
Calcite	4.90	2.00
SRR#1	18.82	7.0
SRR#2	87.86	1.5
PSR#1	5.99	22.0
PSR#2	3.57	36.9
PSR#3	22.7	5.8
PSR#4	29.28	4.5

Note: surface area and site densities for quartz and albite by [31,35], illite from [33], montmorillonite (edge surface only) by [40], and surface area and site density from [34,42]. For the SRR and PSR, the site densities and the effective surface area were calculated based on their mineralogical compositions using Equations (5) and (6), respectively.

It is worth noting that the site densities of minerals such as calcite, quartz, illite, etc. have been reported in literature. However, the equivalent site densities of reservoir rocks and mineral mixtures used in this study have not been reported in literature. Hence, the site densities of SRR and PSR were calculated based on the site densities of the individual mineral constituting the rock (SD_i), the surface area of the individual mineral (A_i), and the effective surface area of the rock (A_{eff}) as given by the Equation:

$$\text{Site density of SRR or PSR}\left(\text{site/nm}^2\right) = \frac{\sum_{\text{a}}^{\text{z}} SD_i\left(\frac{\text{site}}{\text{nm}^2}\right) \times A_i\ \left(\text{m}^2/\text{g}\right)}{\text{Effective Surface Area of Rock,}\ \ A_{eff}\ \left(\text{m}^2/\text{g}\right)} \quad (5)$$

The effective surface area of the SRR and PSR (A_{eff}) was also calculated based on the weight fraction of the individual minerals (w_i) and their surface area (A_i) as given in the Equation:

$$A_{eff}\ \left(\frac{m^2}{g}\right) = \sum_{a}^{z} A_i\ \left(\frac{m^2}{g}\right) \times\ w_i\ (dimensionless) \quad (6)$$

where "a" and "z" depict the first and the last mineralogical constituents in the rock.

The effective surface area (A_{eff}) (Table 5) and the oil site densities (Table 6) were calculated using Equations (3) and (4), respectively. NB. Equation (4) assumes effective surface areas of the rock (mineral mixtures) and respective oil surface to be the same.

Table 6. Estimated oil site densities of the STO used.

Mineral (Rock) Surface	Equivalent Oil Surface	STO#1 Site Density (Site/nm^2)	STO#2 Site Density (Site/nm^2)
Quartz	>COOH >NH$^+$	0.89 16.99	3.40 20.56
Albite	>COOH >NH$^+$	0.89 16.99	3.40 20.56
Illite	>COOH >NH$^+$	0.02 0.31	0.06 0.37
Montmorillonite	>COOH >NH$^+$	0.36 6.79	1.36 8.23
Calcite	>COOH >NH$^+$	0.54 10.20	2.04 12.34
SRR#1	>COOH >NH$^+$	0.15 2.89	0.58 3.50

Table 6. *Cont.*

Mineral (Rock) Surface	Equivalent Oil Surface	STO#1 Site Density (Site/nm^2)	STO#2 Site Density (Site/nm^2)
SRR#2	>COOH >NH$^+$	0.73 13.85	2.77 16.76
PSR#1	>COOH >NH$^+$	0.05 0.93	0.19 1.12
PSR#2	>COOH >NH$^+$	0.03 0.55	0.11 0.67
PSR#3	>COOH >NH$^+$	0.19 3.52	0.70 4.27
PSR#4	>COOH >NH$^+$	0.24 4.51	0.90 5.46

3. Results

In this study, SCM was utilized to predict the wetting state by analyzing the oil adhesion as a result of electrostatic pair linkages formed during rock, brine, and oil interactions. The simulation results during FWI and CWI for minerals were used to investigate the change of wetting preferences for the individual minerals with CW. Moreover, simulations with FWs were taken as references because it was assumed that the reservoirs were initially filled with FW. Furthermore, the interactions between mineral–brine and oil–brine that caused the oil adhesion onto the mineral surfaces were also determined by SCM. Only the dominant interactions are presented in the plots, as less important interactions with less importance had minimal impact on the wetting state of the minerals. Then, identical procedures were used for the reservoir rocks and subsequently mineral mixtures (SRR and PSR).

Four different fluid systems were used in the simulation (FW#1-STO#1, FW#2-STO#1, FW#1-STO#2, and FW#2-STO#2). It is the average results for these fluid systems that are discussed, even though the results are shown for the individual fluid systems.

3.1. Minerals

3.1.1. Total Bond Product

i. Formation Water

The TBP can be used to predict the likelihood of oil adhesion. Figure 2 shows the *TBP* for individual minerals with FW. SCM results showed that quartz is very water-wet (max *TBP* < 0.1). On the other hand, calcite is very oil-wet (minimum *TBP* > 0.8). It can be observed that montmorillonite was more oil-wet than illite, quartz, and albite. Therefore, in the presence of FW, the oil-wetting preference of the minerals were: calcite > montmorillonite > illite > albite > quartz.

ii. Carbonated Water

During CWI, some changes in the minerals' TBP could be observed. The results in Figure 3 demonstrate that calcite was predicted to not be as strongly oil-wet (max *TBP* < 0.4) as in FW, while quartz and albite were predicted to be more water-wet compared to results with FW (Figure 1). Nevertheless, the wettability states of the illite and montmorillonite did not change strongly during CWI. The growing order of the average mineral hydrophobicity also altered slightly, where illite and montmorillonite replaced each other; quartz < albite < montmorillonite < illite < calcite.

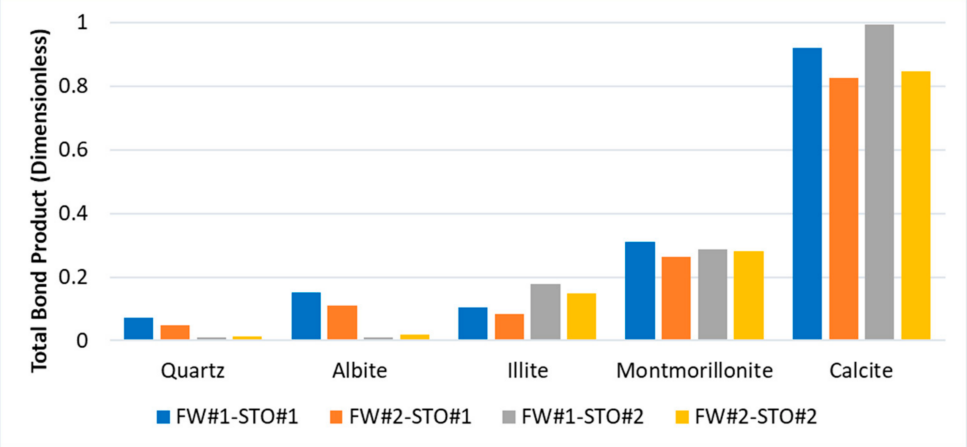

Figure 2. Total bond product (oil adhesion tendency) of minerals during FWI.

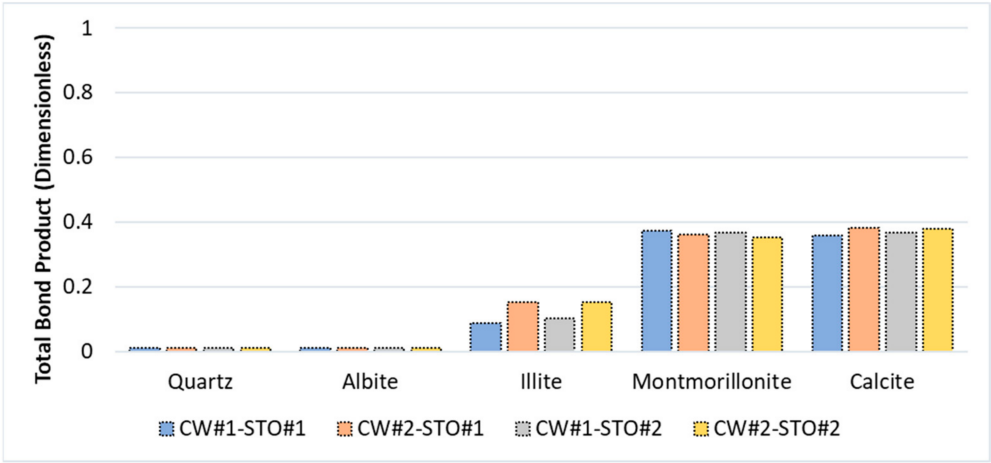

Figure 3. Total bond product (oil adhesion tendency) of minerals during CWI.

3.1.2. Oil adhesion mechanisms in calcite

Compared to other minerals, calcite had the most significant change in wettability preferences after applying CW. Therefore, the bond products of the most dominant interactions in the oil adhesion mechanisms onto calcite during FWI and CWI are demonstrated in this chapter.

i. Formation Water

Figure 4 illustrates that the wettability state of the calcite during FWI was strongly oil-wet. This is mainly due to the high BP for the interaction $> CaOH_2^+ \boxed{\leftrightarrow} > COO^-$ (≈0.43–0.63). Moreover, the cation bridging by divalent cations (Ca^{2+}, Mg^{2+}) also could be observed in oil adhesion mechanisms for calcite. In addition, the impact of the basic component ($>NH^+$) in the oil adhesion mechanisms was small in comparison with the acidic component ($>COO^-$).

ii. Carbonated Water

The change of BP for dominant electrostatic pair linkages before (max BP ≈ 0.6) and after CW (max *BP* ≈ 0.3) showed that CW altered the wettability of calcite. The decrease in the BPs affected the wettability preferences of calcite towards less oil-wet (Figure 4). From Figure 5 it can be observed that during CWI, the electrostatic pair linkage occurred by the cation bridging by divalent cation ($> CO_3^- \boxed{\leftrightarrow} > COOCa^+$) had the largest alteration. The less adhesion was due to the lower concentration of carbonate and carboxylate groups at lower pH.

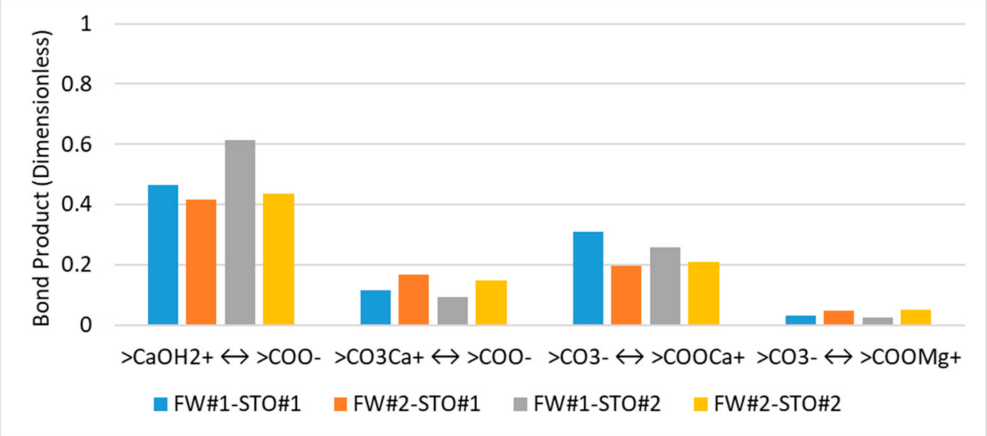

Figure 4. Bond product (oil adhesion mechanism) of calcite during FWI.

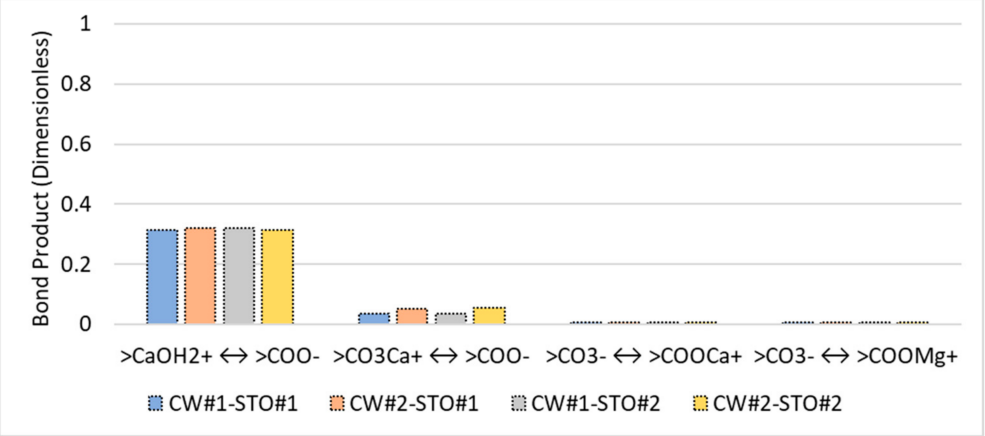

Figure 5. Bond product (oil adhesion mechanism) of calcite during CWI.

3.2. Reservoir Rocks and Mineral Mixtures

In this section, the total bond products for the reservoir rocks and mineral mixtures with FWs and CWs are first presented before the dominating oil adhesion mechanisms are discussed.

3.2.1. Total Bond Product

i. Formation Water

From both the sandstone reservoir rocks (SRR) and the pseudo-sandstone rocks (PSR) simulation results with FWs (Figure 6), it could be observed that the surface area and wetting state of the individual minerals dictates the wetting preferences of the rocks. For instance, the wettability of the PSR#1 and PSR#2 was dominated by their effective surface area (21.98 m^2/g and 36.92 m^2/g, respectively). Nevertheless, the mass fraction of PSR#1 was dominated by quartz (62.8%) while that of PSR#2 was dominated by illite (54.4%). Since both quartz and illite were estimated to be hydrophilic (Figure 2), the wetting states of PSR#1 and PSR#2 were as expected similar to the wetting preferences of the mineral with the largest effective surface area (illite). The effective surface areas of PSR#3 and PSR#4 were also dominated by illite (4.40 m^2/g and 2.94 m^2/g, respectively). In PSR#3, the dominant mass fractions of the minerals were quartz (62.8%) and calcite (25.2%) while in PSR#4, calcite (50.2%) and quartz (41.9%) were the dominant mass fractions. Although the surface area and the mass fraction of the PSR#3 were dominated by hydrophilic minerals (illite and quartz), the wetting state of PSR#3 was observed to be less hydrophilic as compared to SRR#1. This was linked to the high contents of calcite in PSR#3 as compared to SRR#1 (Table 1). On the other hand, though the effective surface area of PSR#4 was dominated by

illite, the simulation results (Figure 6) depicted a relatively high oil-wet state. This showed that the calcite content had a stronger influence on the wetting state of sandstone reservoir rock than the clay minerals.

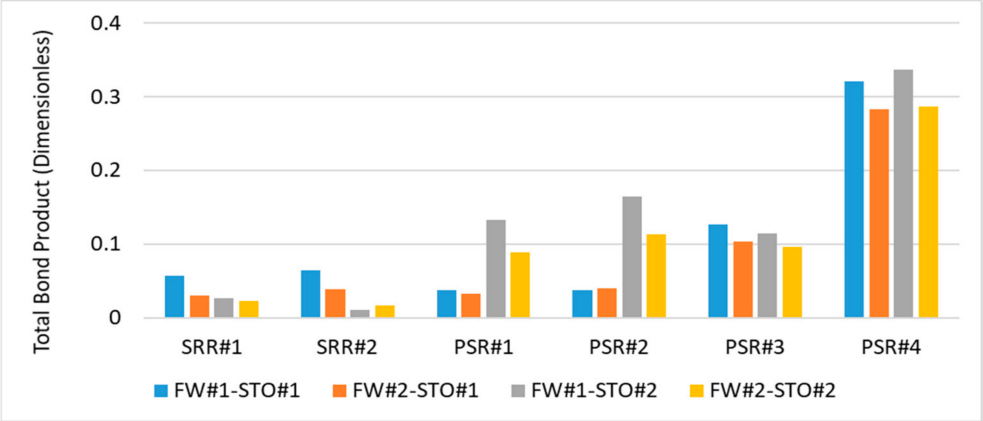

Figure 6. Total bond product (oil adhesion tendency) of reservoir rocks and mineral mixtures during FWI.

ii. Carbonated water

During CWI, the wettability states of the reservoir rocks (SRR#1 and SRR#2) and mineral mixtures (PSR#1, PSR#2, PSR#3, and PSR#4) were altered. Figure 7 illustrates that the wettability state of SRR#1 on average became a bit more oil-wet as illite had the dominating surface area, which has more BPs with cationic oil surfaces during CWI. PSR#1 and PSR#2 also had similar results due to the surface area being dominated by illite. Wettability was changed directly toward more water-wet after applying CW for SRR#2. This was due to the surface area of SRR#2 being dominated by quartz. The wettability preference of the quartz altered towards more water-wet after applying CW at the studied conditions. The wettability states for PSR#3 and PSR#4 were changed from oil-wet to water-wet due to the significant amount of calcite which was changed to more water-wet.

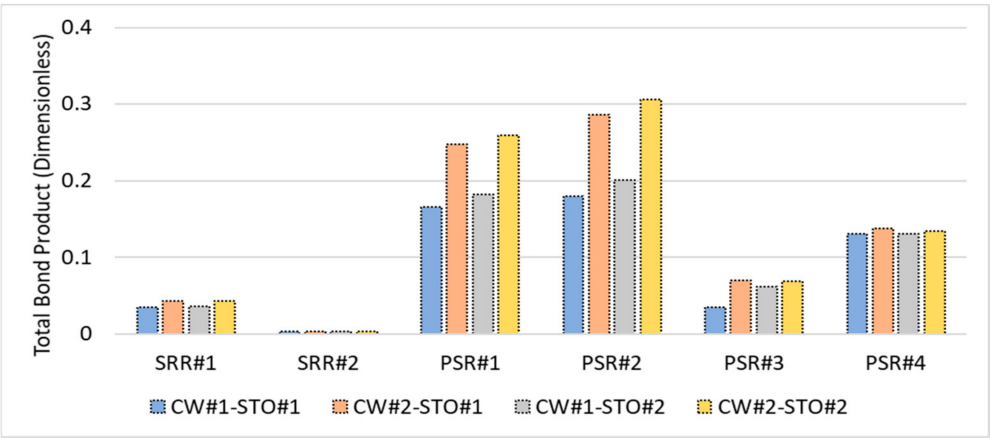

Figure 7. Total bond product (oil adhesion tendency) of reservoir rocks and mineral mixtures during CWI.

3.2.2. Oil Adhesion Mechanism in PSR#4

Compared to other reservoir rocks and mineral mixtures, PSR#4 had the most significant change in wettability preferences after applying CW. Therefore, the bond products of the most dominant interactions in the oil adhesion mechanisms onto PSR#4 during FWI and CWI are presented in this chapter.

i. Formation Water

In Figure 8, it is shown that when the FW is in contact with PSR#4, the BP for the dominant pair linkages ($>CaOH_2^+$ ↔ $>COO^-$) was approximately 0.2, proving that higher calcite content in the rock mixture led to a more oil-wet state.

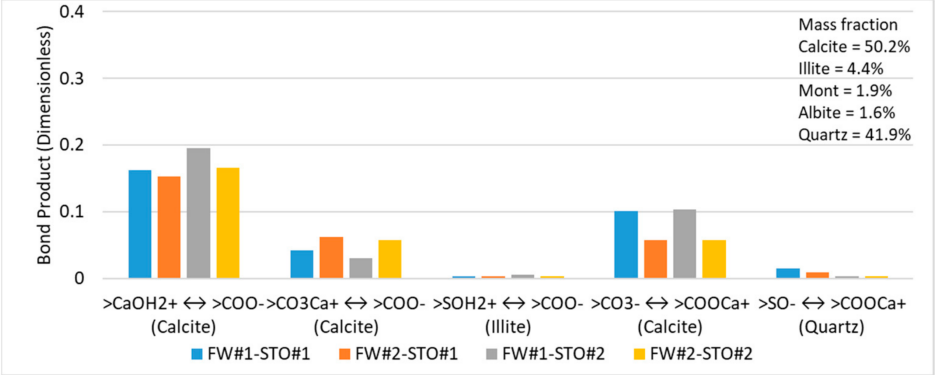

Figure 8. Bond product (oil adhesion mechanism) of PSR#4 during FWI.

ii. Carbonated Water

After applying CW, the pair linkages observed in the mineral mixture (PSR#4) was estimated to be less oil-wet (Figure 9). This was due to the change in BP for electrostatic pair linkages before and after the application of CW. It could be concluded that the wetting state of mineral mixture PSR#4 were made less water-wet after applying CW. This was verified by diminished BP of the main electrostatic linkage from 0.2 to 0.07.

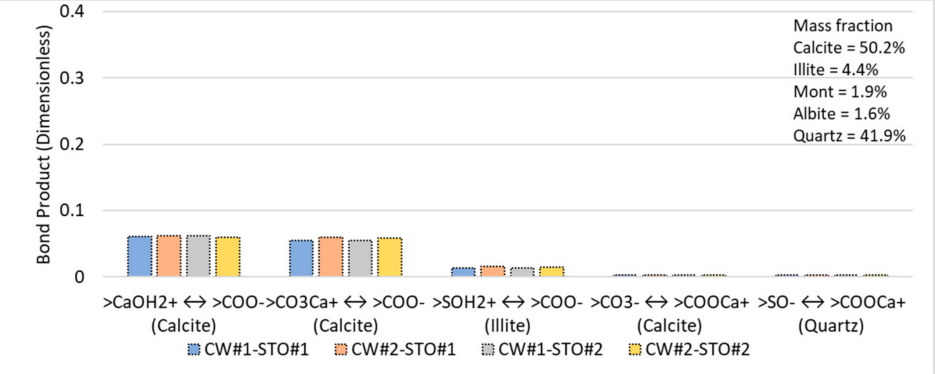

Figure 9. Bond product (oil adhesion mechanism) of PSR#4 using CWI.

4. Discussion

4.1. Prediction of the Wettability with Formation Water

The results of simulation for minerals, reservoir rocks, and mineral mixtures in contact with FWs estimated their wettability states based on the attractive electrostatic forces between the rock-brine and the oil-brine interfaces. The results illustrated that the average wettability states of albite and quartz were toward water-wet while wetting preferences of calcite was strongly oil-wet. Illite and montmorillonite, on the other hand, was intermediate wet when exposed to FW. The ranking of the oil wetness of the studied minerals in FW was calcite > montmorillonite > illite > albite > quartz. From the results of SCM, it could be concluded that the wettability states of rocks were affected by the wetting state and effective surface area of each mineral. The results with FWs were used as a reference for wettability alteration during CWI.

4.2. Prediction of the Wettability during Carbonated Water

The wettability preferences of the same minerals, SRRs, and mineral mixtures, PSRs, were also estimated during CWI. The main reason for the research was to learn more about

the impact of CW on the wetting preferences of the reservoir rocks. The results showed that the wettability states of the albite and quartz were on average changed toward more water-wet during CWI. Nevertheless, the same effects were not observed for the illite and montmorillonite. The wetting state of clay minerals altered on average towards slightly more water-wet and more oil-wet after applying CW, respectively. A noticeable alteration in wetting preference during CWI was estimated for calcite. The wettability of calcite was estimated to be changed from strongly oil-wet toward intermediate-wet or slightly water-wet. This is consistent with a recent study [25] of carbonated water in calcite where it was also observed in contact angle experiments and SCM study that CW altered the calcite towards more water-wet state.

4.3. Limitations

The presented SCM method has several limitations in the estimation of wettability by the geochemical simulator PHREEQ-C. Two important limitations are given below.

4.3.1. Mineral Distribution

A limitation in the SCM results is that the effects of the contacted surface area in the sandstone rocks were not considered. The SCM estimates the wettability by assuming that all the reactive mineral surfaces can take part in the interactions. This may not be the case, as mineral surfaces may be dominated by asperities or surface features [43,44] which may influence the wetting behavior. A possible solution can be to conduct the simulations using the surface area of the individual minerals in direct contact with the flowing fluid. Simulations including contacted surface can be compared with USBM experiments with reservoir fluids since they both take into account mineral distribution and can be carried out with CW. Other experimental methods like Amott tests and floatation cannot be performed with CW.

4.3.2. Surface Precipitation

SCM does not consider the effect of surface precipitation. Depending on the studied recovery process, some crude oils can change their ability to act as solvents for polar oil components due to change in temperature, pressure, or composition. Subsequent precipitation of polar oil components on mineral and rock surfaces can lead to wettability alteration of the surfaces towards less water-wet.

5. Conclusions

The presented paper showed that the SCM technique can predict the tendency for wettability alteration of the individual minerals and reservoir rocks during CWI using the geochemical simulator PHREEQ-C with different brine and STO compositions.

The SCM method is a fast and low-cost technique of predicting the wetting state of the minerals and reservoir rocks by use of a geochemical simulator, PHREEQ-C. The advantage of the SCM technique over other wettability prediction techniques (e.g., the Amott and the USBM) is that this method can predict the dominating oil adhesion mechanisms, such as direct adhesion of carboxylate (>COO^-) and cation bridging. Moreover, the SCM technique can be utilized in the estimation of laboratory experiments. It can also be used as the primary screening tool to predict potential wettability change of reservoir rocks. Then, further evaluation of potential should be accomplished in laboratory reservoir simulations and experiments.

Based on the SCM results, the order of the dominant average minerals oil-wetness at FW was predicted as calcite > montmorillonite > illite > albite > quartz. After applying CW, wettability states of the calcite, illite, albite, and quartz were changed towards more water-wet.

From the SCM results, it can also be seen that the wetting preference of the PSRs and SRRs depended on the effective surface area and wetting preference of the individual minerals except for rocks with high amount of calcite. Therefore, calcite had a more

significant effect on the wetting preferences of the studied sandstone rocks than the other minerals, as electrostatic pair linkage between mineral and oil is more significant for calcite than other studied minerals. Furthermore, the wettability change after applying CW also depended on the effective surface areas and wetting preferences of the individual minerals. Hence, the wettability states of the rocks was largely dictated by the wetting preferences of the dominant mineral during CWI.

Author Contributions: Conceptualization, I.F., S.E., A.O. and F.M.; methodology, I.F. and S.E.; validation, I.F. and A.O.; investigation, I.F., S.E., and F.M.; writing—original draft preparation, I.F., S.E., A.O., and F.M.; writing—review and editing, I.F. and S.E.; visualization, F.M.; supervision, I.F. and A.O.; project administration, I.F. All authors have read and agreed to the published version of the manuscript.

Funding: The presented research was funded by the National IOR Center of Norway and NORCE Norwegian Research Centre AS.

Institutional Review Board Statement: Not applicable.

Informed Consent Statement: Not applicable.

Data Availability Statement: Not applicable.

Acknowledgments: The authors acknowledge NORCE Norwegian Research Centre AS, the Research Council of Norway and the industry partners; ConocoPhillips Skandinavia AS, Aker BP ASA, Vår Energi AS, Equinor ASA, Neptune Energy Norge AS, Lundin Norway AS, Halliburton AS, Schlumberger Norge AS, Wintershall DEA, of The National IOR Centre of Norway for support.

Conflicts of Interest: The authors declare no conflict of interest.

References

1. Craig, F. *The Reservoir Engineering Aspects of Waterflooding*; Spe Monograph Series; Society of Petroleum Engineers: Richardson, TX, USA, 1971; Volume 3, ISBN 978-0895202024.
2. Lake, L.W.; Johns, R.; Rossen, B.; Pope, G. *Fundamentals of Enhanced Oil Recovery*; Society of Petroleum Engineers: Richardson, TX, USA, 2014; ISBN 978-1-61399-328-6.
3. Anderson, W. Wettability Literature Survey-Part 2: Wettability Measurement. *J. Pet. Technol.* **1986**, *38*, 1246–1262. [CrossRef]
4. Donaldson, E.C.; Thomas, R.D.; Lorenz, P.B. Wettability Determination and Its Effect on Recovery Efficiency. *Soc. Pet. Eng. J.* **1969**, *9*, 13–20. [CrossRef]
5. Dubey, S.T.; Doe, P.H. Base Number and Wetting Properties of Crude Oils. *SPE Reserv. Eng.* **1993**, *8*, 195–200. [CrossRef]
6. Mwangi, P.; Thyne, G.; Rao, D. Extensive Experimental Wettability Study in Sandstone and Carbonate-Oil-Brine Systems: Part 1—Screening Tool Development. In Proceedings of the International Symposium of the Society of Core Analysts, Napa Valley, CA, USA, 16–19 September 2013; pp. 1–6.
7. Erzuah, S.; Fjelde, I.; Omekeh, A.V. Wettability Characterization Using the Flotation Technique Coupled with Geochemical Simulation. In Proceedings of the IOR NORWAY 2017—19th European Symposium on Improved Oil Recovery: Sustainable IOR in a Low Oil Price World, Stavanger, Norway, 24–27 April 2017.
8. Fjelde, I.; Omekeh, A.V.; Sokama-Neuyam, Y.A. Low Salinity Water Flooding: Effect of Crude Oil Composition. In *Proceedings of the SPE Improved Oil Recovery Symposium; Tulsa, OK, USA, 12–16 April 2014*; Society of Petroleum Engineers: Richardson, TX, USA, 2014; Volume 2.
9. Mamonov, A.; Kvandal, O.A.; Strand, S.; Puntervold, T. Adsorption of Polar Organic Components onto Sandstone Rock Minerals and Its Effect on Wettability and Enhanced Oil Recovery Potential by Smart Water. *Energy Fuels* **2019**, *33*, 5954–5960. [CrossRef]
10. Fjelde, I.; Asen, S.M. Wettability Alteration During Water Flooding and Carbon Dioxide Flooding of Reservoir Chalk Rocks. In Proceedings of the SPE EUROPEC/EAGE Annual Conference and Exhibition, Barcelona, Spain, 14–17 June 2010.
11. Dong, Y.; Dindoruk, B.; Ishizawa, C.; Lewis, E.; Kubicek, T. An Experimental Investigation of Carbonated Water Flooding. In Proceedings of the SPE Annual Technical Conference and Exhibition, Denver, CO, USA, 30 October–2 November 2011.
12. Grape, S.; Poston, S.; Osoba, J. Imbibition Flooding with CO2-Enriched Water. In Proceedings of the SCA Annual technical conference, Dallas, TX, USA, 14–16 August 1990.
13. Kechut, N.I.; Sohrabi, M.; Jamiolahmady, M. SPE 143005 Experimental and Numerical Evaluation of Carbonated Water Injection (CWI) for Improved Oil Recovery and CO2 Storage. In Proceedings of the SPE EUROPEC/EAGE Annual Conference and Exhibition, Vienna, Austria, 23–26 May 2011.
14. Sohrabi, M. Coreflooding Studies to Investigate the Potential of Carbonated Water Injection as an Injection Strategy for Improved Oil Recovery and CO2 Storage. *Transp. Porous Media* **2011**, *91*, 101–121. [CrossRef]

15. Riazi, M.; Sohrabi, M.; Jamiolahmady, M. Experimental Study of Pore-Scale Mechanisms of Carbonated Water Injection. *Transp. Porous Media* **2010**, *86*, 73–86. [CrossRef]
16. Teklu, T.W. Low-salinity water-alternating-CO2 EOR. *J. Pet. Sci. Eng.* **2016**, *142*, 101−118. [CrossRef]
17. Seyyedi, M. Quantification of oil recovery efficiency, CO2 storage potential, and fluid-rock interactions by CWI in heterogeneous sandstone oil reservoirs. *J. Mol. Liq.* **2018**, *249*, 779–788. [CrossRef]
18. Potter, G.F. The Effects of CO2 Flooding on Wettability of West Texas Dolomitic Formations. In Proceedings of the Society of Petroleum Engineers, Dallas, TX, USA, 27–30 September 1987.
19. Seyyedi, M.; Sohrabi, M.; Farzaneh, A. Investigation of Rock Wettability Alteration by Carbonated Water through Contact Angle Measurements. *Energy Fuels* **2015**, *29*, 5544–5553. [CrossRef]
20. Brady, P.V.; Krumhansl, J.L. A surface complexation model of oil-brine-sandstone interfaces at 100 °C: Low salinity waterflooding. *J. Pet. Sci. Eng.* **2012**, *81*, 171–176. [CrossRef]
21. Sanaei, A.; Tavassoli, S.; Sepehrnoori, K. Investigation of modified Water chemistry for improved oil recovery: Application of DLVO theory and surface complexation model. *Colloids Surfaces A Physicochem. Eng. Asp.* **2019**, *574*, 131–145. [CrossRef]
22. Korrani, A.K.N.; Jerauld, G.R. Modeling wettability change in sandstones and carbonates using a surface-complexation-based method. *J. Pet. Sci. Eng.* **2019**, *174*, 1093–1112. [CrossRef]
23. Yutkin, M.P.; Lee, J.Y.; Mishra, H.; Radke, C.J.; Patzek, T.W. Bulk and surface aqueous speciation of calcite: Implications for low-salinity waterflooding of carbonate reservoirs. In Proceedings of the SPE Kingdom of Saudi Arabia Annual Technical Symposium and Exhibition, Dammam, Saudi Arabia, 25–28 April 2016; pp. 25–28. [CrossRef]
24. Ding, H.; Mettu, S.; Rahman, S.S. Impacts of Smart Waters on Calcite-Crude Oil Interactions Quantified by "soft Tip" Atomic Force Microscopy (AFM) and Surface Complexation Modeling (SCM). *Ind. Eng. Chem. Res.* **2020**, *59*, 20337–20348. [CrossRef]
25. Chen, Y.; Sari, A.; Xie, Q.; Saeedi, A. Insights into the wettability alteration of CO 2 -assisted EOR in carbonate reservoirs. *J. Mol. Liq.* **2019**, *279*, 420–426. [CrossRef]
26. Xie, Q.; Sari, A.; Pu, W.; Chen, Y.; Brady, P.V.; Al Maskari, N.; Saeedi, A. pH effect on wettability of oil/brine/carbonate system: Implications for low salinity water flooding. *J. Pet. Sci. Eng.* **2018**, *168*, 419–425. [CrossRef]
27. Erzuah, S.; Fjelde, I.; Omekeh, A.V. Wettability Estimation using surface-Complexation Simulations. *SPE Reserv. Eval. Eng.* **2019**, *22*, 509–519. [CrossRef]
28. Mahani, H.; Keya, A.L.; Berg, S.; Nasralla, R. Electrokinetics of carbonate/brine interface in low-salinity waterflooding: Effect of brine salinity, composition, rock type, and pH on ζ-potential and a surface-complexation model. *SPE J.* **2017**, *22*, 53–68. [CrossRef]
29. Buckley, J.S.; Liu, Y.; Monsterleet, S. Mechanisms of Wetting Alteration by Crude Oils. *SPE J.* **1998**, *3*, 54–61. [CrossRef]
30. Koretsky, C. The Significance of Surface Complexation Reactions in Hydrologic Systems: A Geochemist's Perspective. *J. Hydrol.* **2000**, *230*, 127–171. [CrossRef]
31. Sverjensky, D.A.; Sahai, N. Theoretical Prediction of Single-Site Surface-Protonation Equilibrium Constants for Oxides and Silicates in Water. *Geochim. Cosmochim. Acta* **1996**, *60*, 3773–3797. [CrossRef]
32. Brady, P.V.; Krumhansl, J.L.; Mariner, P.E. Surface Complexation Modeling for Improved Oil Recovery. In Proceedings of the SPE Symposium on Improved Oil Recovery, Tulsa, Oklahoma, USA, 14–18 April 2012; pp. 14–18.
33. Gu, X.; Evans, L.J. Modelling the Adsorption of Cd (II), Cu (II), Ni (II), Pb (II), and Zn (II) onto Fithian Illite. *J. Colloid Interface Sci.* **2007**, *307*, 317–325. [CrossRef]
34. Wolthers, M.; Charlet, L.; Van Cappellen, P. The surface chemistry of divalent metal carbonate minerals: A critical assessment of surface charge and potential data using the charge distribution multi-site ion complexation model. *Am. J. Sci.* **2008**, *308*, 905–941. [CrossRef]
35. Sverjensky, D.A.; Sahai, N. Theoretical prediction of single-site enthalpies of surface protonation for oxides and silicates in water. *Geochim. Cosmochim. Acta* **1998**, *62*, 3703–3716. [CrossRef]
36. Brady, P.V.; Morrow, N.R.; Fogden, A.; Deniz, V.; Loahardjo, N.; Winoto, A. Electrostatics and the low salinity effect in sandstone reservoirs. *Energy Fuels* **2015**, *29*, 666–677. [CrossRef]
37. Erzuah, S. Wettability Estimation by Oil Adsorption. Ph.D. Thesis, University of Stavanger, Stavanger, Norway, 2019.
38. Mehdiyev, F. Surface Complexation Modelling of Wettability Alteration during Carbonated Water Flooding. Master's Thesis, Univesity of Stavanger, Stavanger, Norway, 2021.
39. *Surface Complexation Modelling*, 1st ed.; Lützenkirchen, J. (Ed.) Elsevier: Amsterdam, The Netherlands, 2006.
40. Wieland, E.; Wanner, H.; Albinsson, Y. *A Surface Chemical Model of the Bentonite-Water Interface and Its Implications for Modelling The Near Field Chemistry*; Report SKB-95-26; Swedish Nuclear Fuel and Waste Management Co.: Stockholm, Sweden, 1995.
41. Schmatz, J.; Urai, J.L.; Berg, S.; Ott, H. Nanoscale imaging of pore-scale fluid-fluid-solid contacts in sandstone. *Geophys. Res. Lett.* **2015**, *42*, 2189–2195. [CrossRef]
42. Hjuler, M.; Fabricius, I.L. Engineering Properties of Chalk Related to Diagenetic Variations of Upper Cretaceous Onshore and offshore Chalk in the North Sea Area. *J. Pet. Sci. Eng.* **2009**, *68*, 151–170. [CrossRef]
43. Hilner, E.; Andersson, M.P.; Hassenkam, T.; Matthiesen, J.; Salino, P.A.; Stipp, S.L.S. The effect of ionic strength on oil adhesion in sandstone—The search for the low salinity mechanism. *Sci. Rep.* **2015**, *5*, 1–9. [CrossRef]
44. Hassenkam, T.; Matthiesen, J.; Pedersen, C.S.; Dalby, K.N.; Stipp, S.L.S.; Collins, I.R. Observation of the low salinity effect by atomic force adhesion mapping on reservoir sandstones. *Proc.-SPE Symp. Improv. Oil Recover.* **2012**, *1*, 716–729. [CrossRef]